Nano mechanical properties on the mineralogical array of calcium silicate hydrates and calcium hydroxide through molecular dynamics—CSIR–SERC

B. Bhuvaneshwari[1], G. S. Palani[1], R. Karunya[1] and Nagesh R. Iyer[2],*

[1]CSIR-Structural Engineering Research Centre, Chennai 600 113, India
[2]Academy of Scientific & Innovative Research, Chennai 600 113, India

Molecular dynamics studies towards assessing the bulk properties of the mineralogical array of cement hydrates such as calcium silicate hydrates (C-S-H) and calcium hydroxide (CH) have been conducted. In the case of C-S-H, closely related structures of minerals such as Tobermorite (9, 11, 14) Å and Jennite are taken for MD simulations, as they have similarities with C-S-H in terms of its mineralogical array. COMPASS force field with appropriate set parameters such as cut-off distances, micro-canonical ensembles was employed for the smooth running of simulations. Different supercells for the mineral systems were created and studied further. Results show the calculated mechanical properties of cement hydrates, which form an important input for developing computational model for cement hydrate systems for assessing the physico-chemical and mechanical characteristics.

Keywords: Cement hydrate, force field, mechanical characteristics, molecular dynamics.

CEMENT industry is one of the major global contributors to carbon dioxide emission. It accounts for an estimated 5–8% of the world's CO_2 emission and consumes 26% of the total required energy towards particle grinding[1]. The strength and durability of the cement rely upon the organization of cement nanoparticles[2] as the dimensions of hydration products of cement are roughly between 1 and 100 nm. The reduction in CO_2 emission can be achieved or controlled either by proper usage of supplementary cementitious materials as cement replacement or by controlling/modifying the properties of CO_2-emitting constituent in the cement clinker itself. Understanding and interpreting the chemical and microstructural phenomenon through characterizing cement hydration process are quite complex and interdependent, and also making it difficult to resolve the individual mechanisms or parameters that determine their rates. Based on the literature review, it is observed that only limited experimental works are available on the mechanical properties of cement hydrate phases, mainly calcium silicate hydrate (C-S-H) and Portlandite or calcium hydroxide (CH)[3,4]. Dormieux and Ulm[5] used nanoindentation technique and microporomechanics theories to indirectly calculate the solid phase elastic modulus. It is relatively difficult to perform direct mechanical testing to measure the properties of the solid C-S-H and only limited works are reported in the literature[6]. Computational simulations were carried out to enhance materials design, which include electronic structure calculations, molecular dynamics, Monte Carlo and continuum methods, as well as multiscale combination of methods[1,7]. Molecular dynamics (MD) and Lattice dynamics simulations are often used to calculate the electronic, spectroscopic and mechanical properties of clinker and hydrate phases[8–10]. Studies towards atomic structure–property relationships are an emerging area of research due to the increasingly significant environmental, social and economic impact of the global Portland cement usage and production, which currently stands at 2 billion metric tonnes[8].

C-S-H: a nano particulate of cement hydrates

The hydration of cement is a complicated phenomenon and not easy to understand due to the complexity in chemical composition of different batches of cement. The water involved in hydration will be classified into three types such as gel water, physically adsorbed water and chemically bound water. Calcium silicate hydrate, the main product in Portland cement hydration, influences the physical and mechanical properties of most cementitious materials. C-S-H has a structural multiscale organization formed by agglomerated particles or nanocrystallites composed of stacked lamellae formed by a double central layer of CaO octahedra inserted between two layers of SiO_4 tetrahedra, which are linked with a periodicity of three tetrahedral chains called dreierketten[11]. The milestone work done by Powers and Brownyard[6] is the first step in revealing the nano particulate structure of C-S-H

and cement gel. This was taken forward by many other researchers worldwide[3,6]. Though there are a several computational models, which relate the nanostructural features of C-S-H, unfortunately, currently there is no literature with detailed report of real C-S-H structure. Structure-related C-S-H crystals, i.e. Tobermorite and Jennite were recently studied by Bonaccorsi *et al.*[12,13]. The molecular or atomic arrangements in Tobermorite 14 Å are shown in Figure 1. Still the grey area is the exact nanostructure of the C-S-H disordered layer structure. However, it is understood that despite the great socio-economic importance and the existence of several proposed models for describing the structure of C-S-H, there are no structural models that currently relate chemical composition, nanostructure, and microstructure with the physico-chemical and mechanical properties[11]. Without this knowledge, it is not possible to understand and control the behaviour of cement-based materials such as creep and shrinkage, which is the most important parameter for durability issues[14].

The overall scenario of the nature of C-S-H in different cementitious environments helps analyse the functions during their participation at a given ratio. Also, it is known that there are at least 30 crystalline minerals that are similar in composition to C-S-H and they differ in atomic arrangement, Ca/Si ratio (0.83 for Tobermorite, 1.8 for Jennite), and the number of –OH and H_2O groups. Therefore, it is important to take research a step deeper into the understanding of relationship between different nanostructural arrangements of minerals. This relates the compositional stability of C-S-H formed in the presence of various mineral admixtures during hydration either through experimental or computational investigations, which may build a platform to find a possible replacement for the calcium in cement powder. Hence, the reduction in the use of cement may be directly achieved by adopting new methods of control, including guidance based on simulation, which dramatically improves the performance of concrete[1,15].

Numerous experimental and computational studies agree that C-S-H nanotexture can be viewed as a mixture of Tobermorite and Jennite structures in which these layered species show multiple imperfections, but the nanoscopic short-ordering structure (1–5 nm) of C-S-H gel remains elusive, as stated by Gonzalez-Teresa *et al.*[16]. This work aims to study the mechanical properties of structurally related minerals of C-S-H such as Tobermorite (Ca/Si – 0.83), Jennite (Ca/Si – 1.8) and Portlandite (CH) through MD simulations. Tobermorite has a monoclinic lattice structure and it is available in three different (layer) thicknesses, namely 9 Å [$Ca_5Si_6O_{16}(OH)_2$], 11 Å [$Ca_5Si_6O_{17} \cdot 5H_2O$ to $Ca_4Si_6O_{15}(OH)_2 \cdot 5H_2O$] and 14 Å [$Ca_5Si_6O_{16}(OH)_2 \cdot 7H_2O$] as characterized by basal spacing[13]. The outcome of the present study can further help in understanding the nanostructural features of cement hydrates in the presence of secondary mineral admixtures through in-depth insight on multiscale modelling of cement hydrates.

Features of molecular dynamics

It is well known in the computational molecular modelling field that MD is characterized as a method of 'particle tracking'. This can be distinguished by two versions, namely classical and *ab initio*, the former for treating atoms as classical entities (position and momentum), and the latter for treating separately the electronic and ionic degrees of freedom, where a wave function description is used for the electrons. MD is one of the modelling schemes of molecular mechanics, which directly calculates the potential energy surface or allows to simulate the time-dependent behaviour of molecular systems by solving classical Newton's laws of motion:

$$-\frac{dE}{dR} = m\frac{d^2R}{dt^2},$$ (1)

where E is the potential energy, R the position of the nuclei, m the mass and t is the time.

As such, MD is an indispensable tool to interpret experimental data. However, the accuracy of MD simulations is intrinsically dependent on the quality of the empirical potential energy functions and the force-field parameters used[17,18]. Here, the nuclei of atoms are considered classically as spheres connected to each other through a set of springs emulating chemical bonds. The motion of the atoms is simulated by the forces acting on each atom, which are derived from a set of force-field parameters. Choosing proper force fields is a crucial step in MD simulation. The average description of the existing interactions among various atoms in a molecule or a group of molecules which has a set of functions and parameters in molecular mechanics and MD is called as force field. The potential energy functions of the atoms or molecules (force field) are described based on eq. (2) below. Unfortunately there is no guidance to choose a right force field for the simulation of hydrated cement materials; therefore, it is desirable to try different available force fields[6]. Also, MD integrates iteratively and numerically the classical equations of motion for every atom in the system at time increments (Δt, time step) that are user-defined. For this purpose, a number of algorithms exist that are implemented in different computational codes[19,20]

$$V(r^N) = \sum_{\text{bonds}} \frac{K_i}{2}(l_i - l_{i,0})^2 + \sum_{\text{angles}} \frac{K_i}{2}(\theta_i - \theta_{i,0})^2$$

$$+ \sum_{\text{bonds}} \frac{V_n}{2}(1 + \cos(n\omega - \gamma))$$

$$+\sum_{i=1}^{N}\sum_{j=i+1}^{N}\left(4\varepsilon_{ij}\left[\left(\frac{\sigma_{ij}}{r_{ij}}\right)^{12}-\left(\frac{\sigma_{ij}}{r_{ij}}\right)^{6}\right]+\frac{q_iq_j}{4\pi\varepsilon_0 r_{ij}}\right)$$

$$+ \text{ cross terms}, \tag{2}$$

where V is the potential energy of the molecular system, i, j are atoms, r^N the coordinates of all atoms, K_i the individual energy terms, l the bond length, θ the valance angle, V_n the height of the torsional barrier $(n\omega - \gamma)$ the torsional angle, q_iq_j the net atomic charges of atoms i, j and r_{ij} is the interatomic distance.

Methods and results

Forcite module of Material Studio (MD) simulation software has been used for all the steps followed in the present study towards mechanical property predictions of cement hydrates. The super cells of $1a \times 1b \times 1c$ and $2a \times 2b \times 2c$ (a, b, c correspond to unit cell dimensions) were created on the cement hydrates or minerals and the corresponding structures were relaxed by adopting the suitable NPT (N, number of atoms, P, pressure, and T, temperature) micro-canonical ensembles. The energy and geometry optimized minerals were chosen as the subject for this study. 'Smart minimization method' was used to optimize the structures with a high energy configuration. The cell parameters were based on crystallographic database. The number of atoms considered for modelling and simulations was limited to 2000. Based on this limitation, the unit cell was formed. Initial check on the convergence criteria was performed by applying static and rapidly converging fluctuation methods, as these are some of the most preferred approaches. The potential energy for COMPASS can be expressed in the following form[21]

$$E_{\text{total}} = \sum_b [K_2(b-b_0)^2 + K_3(b-b_0)^3 + K_3(b-b_0)^4]$$

$$+\sum_\theta [K_{2\theta}(\theta-\theta_0)^2 + K_{3\theta}(\theta-\theta_0)^3 + K_{4\theta}(\theta-\theta_0)^4]$$

$$+\sum_\phi [K_{1\phi}(1-\cos\phi) + K_{2\phi}(1-\cos 2\phi) + K_{3\phi}(1-\cos 3\phi)]$$

$$+\sum_\chi K_{2\chi}(\chi-\chi)^2 + \sum_{b,\theta} K_{b\theta}(b-b_0)(\theta-\theta_0)$$

$$+\sum_{b,\phi}(b-b_0)[K_{1b}\cos\phi + K_{2b}\cos 2\phi + K_{3\phi}\cos 3\phi]$$

$$+\sum_{\theta,\phi}(\theta-\theta_0)[K_{1\theta\phi}\cos\phi + K_{2\theta\phi}\cos 2\phi + K_{3\theta\phi}\cos 3\phi]$$

$$+\sum_{b\theta}(\theta'-\theta'_0)(\theta-\theta_0) + \sum_{\theta,\phi}K_{\theta\phi}(\theta'-\theta'_0)(\theta-\theta_0)\cos\phi$$

$$+\sum_{ij}\frac{q_iq_j}{r_{ij}} + \sum_{ij}\varepsilon_{ij}\left[2\left(\frac{r_{ij}^0}{r_{ij}}\right)^9 - 3\left(\frac{r_{ij}^0}{r_{ij}}\right)^6\right]. \tag{3}$$

Initially, the system is relaxed using NVE (V – volume of the unit cell, E – energy of the unit cell) canonical ensemble to bring the corresponding crystallographic structure of cement hydrates into ground state. The undeformed and optimized structures after satisfying the convergence criteria are subjected to dynamics with NPT canonical ensemble (N – constant number of atoms, P – constant pressure (1 atm (0.0001 GPa)) and T – constant temperature (298 K)) for all the systems. Generally, the time step as 1 fs is suitable for most purposes according to Verlet time-integration method. Depending on the number of atoms in the system, the dynamics time used in the study ranged between 50 and 500 ps.

Following this initial stage on convergence, three tensile and shear deformations were applied to the undeformed systems. The resultant internal stress tensor was then obtained from the analytically calculated virial equation of state (eq. (4)), which was used to obtain estimates of the six columns of the elastic stiffness coefficients matrix.

$$\sigma_{\alpha\beta} = \sum_i \left(\frac{v_a}{\Omega}\right)\sigma_{\alpha\beta}^i, \tag{4}$$

where

$$\sigma_{\alpha\beta}^i = \frac{1}{v_a}\left\langle -mv_{i\alpha}v_{i\beta} + \sum_{j>i}\frac{\partial V(r_{ij})}{\partial r_{ij}}\frac{r_{ij\alpha}r_{ij\beta}}{r_{ij}}\right\rangle,$$

with v_a being average volume of one atom; $v_{i\alpha}$ the α-component of vector V_i and $r_{ij\alpha}$; $r_{ij\alpha}$ the α-component of vector $r_i - r_j$ and $\sigma_{\alpha\beta}^i$ is the atomic level stress in atom i.

Elastic modulus, Poisson's ratio, bulk modulus and shear modulus of the deformed clinker phases were calculated based on the Voigt notations (eqs (5)–(8)). In order to obtain the above factors, simulations were repeated at least 50 times to get meaningful statistical averages.

$$\text{Young's modulus } E = \mu\left(\frac{3\lambda + 2\mu}{\lambda + \mu}\right), \tag{5}$$

Table 1. Unit cell details of C-S-H minerals analogue and calcium hydroxide

Mineral system		Cell length (Å) $a : b : c$	Angles (degrees) $\alpha : \beta : \gamma$
Tobermorite 9 Å Monoclinic	$1a \times 1b \times 1c$ No. of atoms: 196	11.274 : 7.344 : 11.468	99.18 : 97.19 : 90.03
	$2a \times 2b \times 2c$ No. of atoms: 1568	22.548 : 14.688 : 22.936	
Tobermorite 11 Å Monoclinic	$1a \times 1b \times 1c$ No. of atoms: 184	6.735 : 7.385 : 22.487	90 : 90 : 123.25
	$2a \times 2b \times 2c$ No. of atoms: 1472	13.47 : 14.77 : 44.974	
Tobermorite 14 Å Monoclinic	$1a \times 1b \times 1c$ No. of atoms: 240	6.735 : 7.425 : 27.987	90 : 90 : 123.25
	$2a \times 2b \times 2c$ No. of atoms: 1920	13.47 : 14.85 : 55.974	
Jennite Triclinic	$1a \times 1b \times 1c$ No. of atoms: 81	10.576 : 7.265 : 10.931	101.3 : 96.98 : 109.65
	$2a \times 2b \times 2c$ No .of atoms: 648	21.152 : 14.53 : 21.862	
Calcium hydroxide Trigonal	$1a \times 1b \times 1c$ No. of atoms: 5	3.586 : 3.586 : 4.880	90 : 90 : 120
	$2a \times 2b \times 2c$ No. of atoms: 40	7.172 : 7.172 : 9.760	
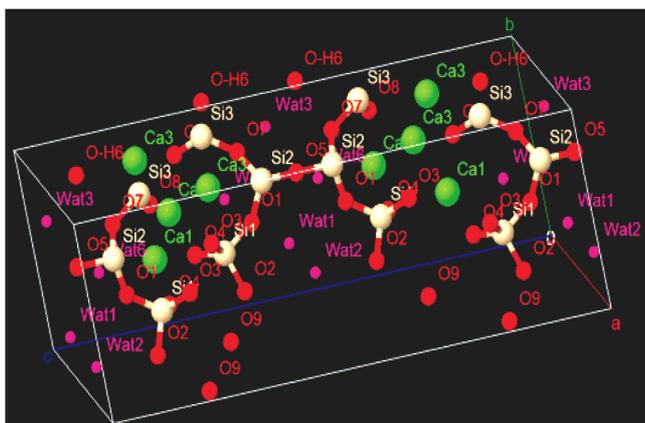
Figure 1. Molecular or atomic arrangements in Tobermorite 14 Å.

Poisson's ratio $v = \dfrac{\lambda}{2(\lambda + \mu)},$ \hfill (6)

Bulk modulus $K = \lambda + \dfrac{2}{3}\mu,$ \hfill (7)

Shear modulus $G = \mu,$ \hfill (8)

where λ is the Lame's modulus and μ the shear modulus.

The unit cell details and projection of cement hydrates (C-S-H minerals analogue and CH) after geometry optimization are shown in Table 1 and Figure 2 and snapshots taken during geometry and energy optimizations of the respective systems are shown in Figure 3. It can be referred from the optimization steps carried out that all the corresponding cement hydrate structures attained the ground state (relaxed) energy before dynamics, which is one of the basic criteria ensuring non-fluctuations in energy states of the systems.

The non-bonded (van der Walls and electrostatic) energy stored in the mineralogical systems before and after dynamics studies was obtained through MD. From the energy results obtained, the root mean square (RMS) force was calculated, as these are important parameters during the dynamics due to the intra-atomic or molecular displacements of atoms or molecules. The calculated mechanical properties such as Young's modulus, Poisson's ratio, bulk modulus and shear modulus of the cement hydrates are shown in Figure 4.

It can be seen from Figure 4 that among the C-S-H nano particulates, namely Tobermorite 9 Å, 11 Å, 14 Å and Jennite, highest bulk properties such as elastic modulus, bulk modulus, shear modulus and Poisson's ratio are achieved by Tobermorite 9 Å. The order of the strengths are as follows: Jennite > Tobermorite 9 Å > Tobermorite 11 Å > Tobermorite 14 Å. The highest strength achieved by Jennite and lowest strength achieved by Tobermorite 14 Å are due to the repeat distance, i.e. 0.5 nm in the former and 1.4 nm in the latter. The reason behind the differential strength among the Tobermorite groups is due to the presence of hydrogen bonds. The layer or array of hydrogen bonds in Tobermorite 14 Å (ref. 13) is shown in Figure 5. Based on the experimental finding on calculating the hydrogen bond distance

Tobermorite 9 Å ($1a \times 1b \times 1c$)

Tobermorite 9 Å ($2a \times 2b \times 2c$)

Tobermorite 11 Å ($1a \times 1b \times 1c$)

Tobermorite 11 Å ($2a \times 2b \times 2c$)

Tobermorite 14 Å ($1a \times 1b \times 1c$)

Tobermorite 14 Å ($2a \times 2b \times 2c$)

Jennite ($1a \times 1b \times 1c$)

Jennite ($2a \times 2b \times 2c$)

Calcium hydroxide ($1a \times 1b \times 1c$)

Calcium hydroxide ($2a \times 2b \times 2c$)
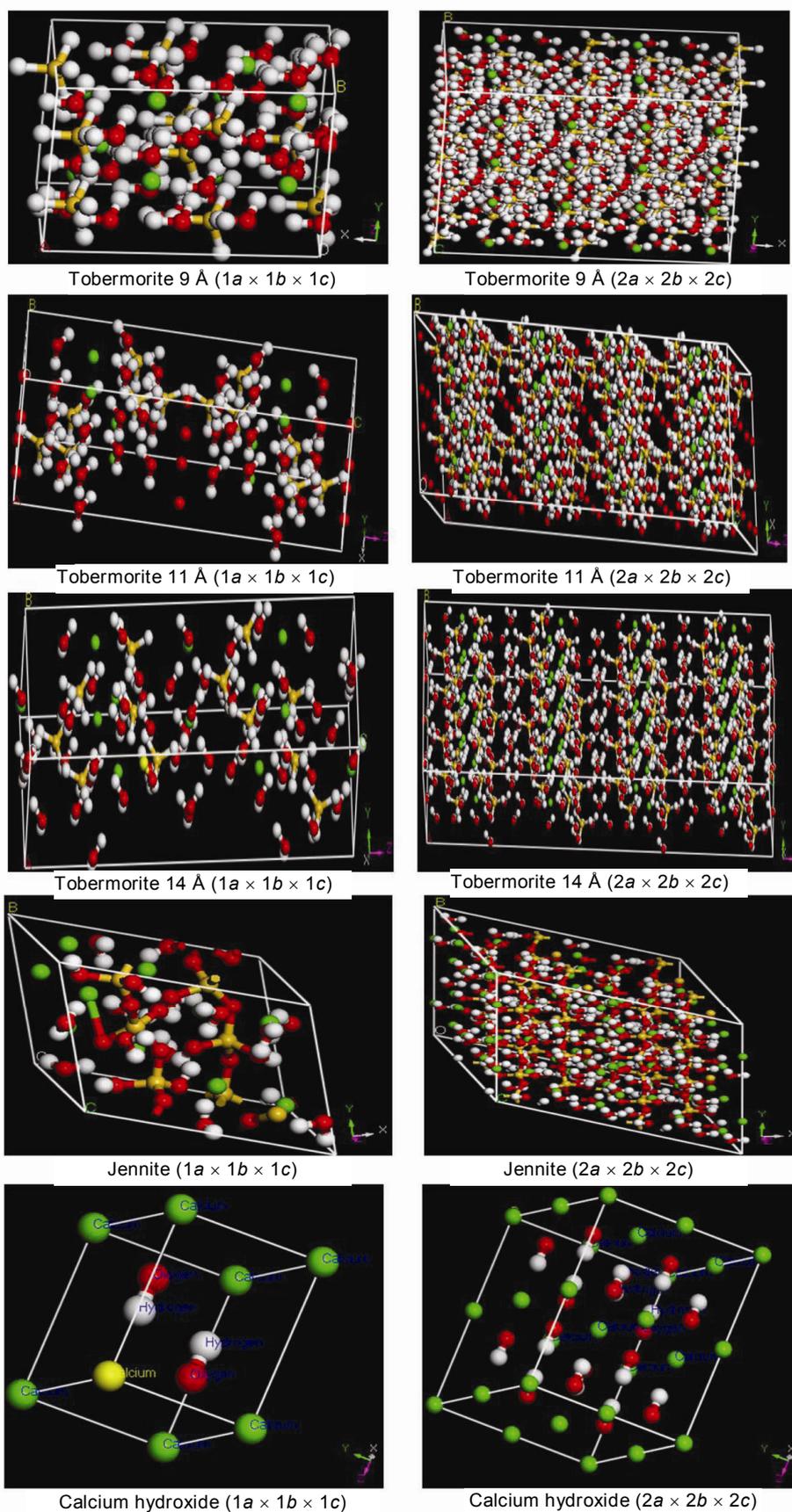
Figure 2. Unit cell projection of cement hydrates after geometry optimization.
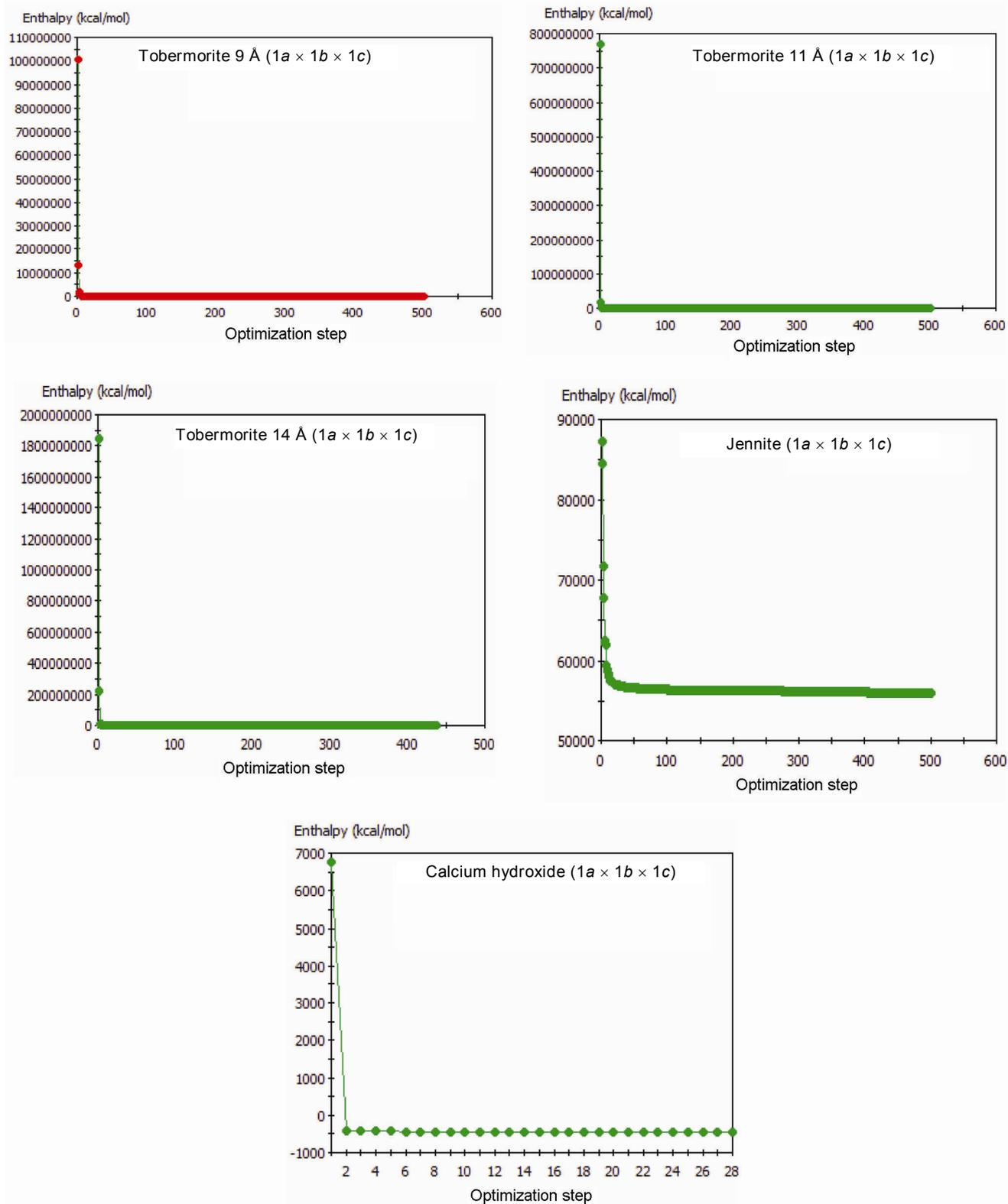
Figure 3. Snapshots of geometry optimization of cement hydrates during molecular dynamics (MD) simulations.

and hydro links (water), it can be inferred that both the bonding parameters play a crucial role in stabilizing the Tobermorite structures. Hence, in the case of Tobermorite

14 Å, the bond layer is much longer compared to its other analogues, which resulted in the least stable structure under stress, as reflected in the decrease in strength. The
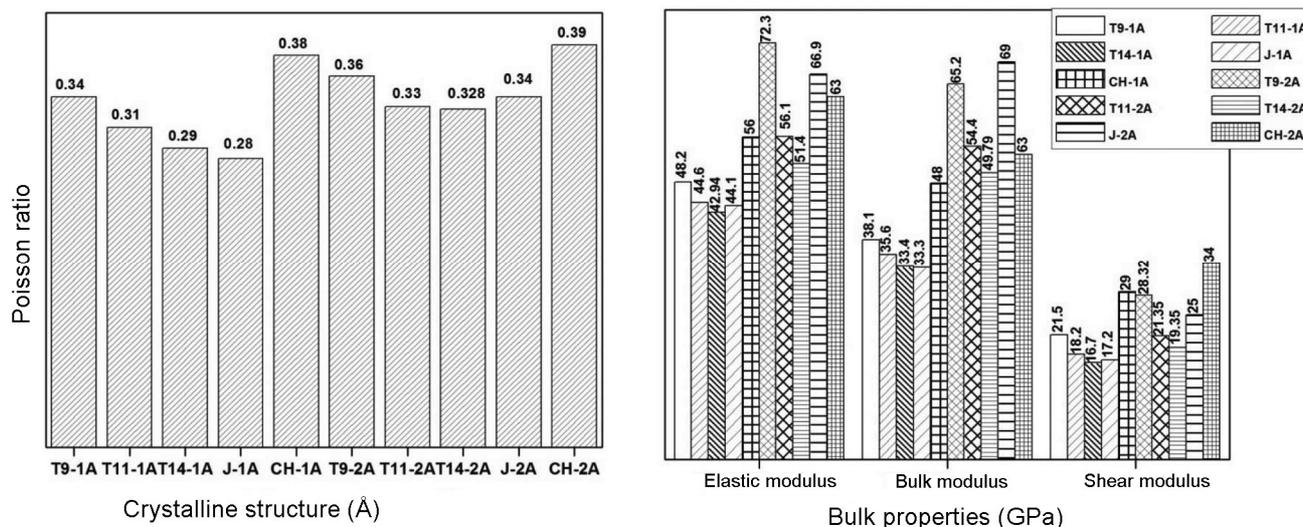
Figure 4. Mechanical or bulk properties of cement hydrates obtained through MD simulations.
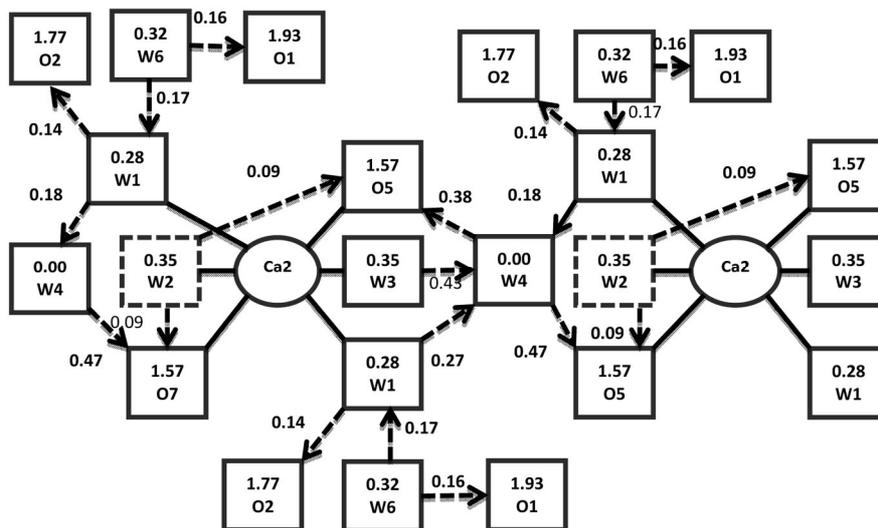
Figure 5. Hydrogen bonding system in Tobermorite 14 Å (dashed arrows indicate the strength of each hydrogen bond).

calculated RMS forces for the supercell consisting of $1a \times 1b \times 1c$ Tobermorite (9, 11, 14) Å analogue are 3.626, 4.249 and 4.627 kcal/mol/Å respectively. It has been proven by RMS forces that due to the least displacement of intra-atoms or molecules of hydrates, Tobermorite 9 Å has the highest bulk property compared to other analogues. RMS forces are not taken for comparison of different mineral structures as the in-built stresses vary with respect to atomic arrangements due to the variable nature of silicate chains and interlayer interactions are dominated by Coulombic forces rather than van der Waals dispersion forces[22]. However, portlandite mineral or CH showed better performance in all aspects compared to C-S-H nano particulates during MD simulations, which is due to the absence of displacement-free

atoms or molecules during dynamics in the CH crystal assembly. The results obtained from the present study are in good agreement with variation of 30–40% with reference to the reported results by Shahsavari et al.[22] and Jorge Dolado and van Breugel[23].

Conclusion

MD simulations are used to calculate bulk properties such as elastic modulus, Poisson's ratio, bulk modulus and shear modulus of cement hydrates, namely C-S-H and CH using different super cells. It can be concluded that the order of the strengths for the cement hydrate systems is as follows: Jennite > Tobermorite 9 Å > Tobermorite 11 Å >

Tobermorite 14 Å with respect to both the supercells created. Thus, this article presents the procedure for multiscale modelling of cementitious composites, which can be a platform for developing computational model for cement hydrate systems for assessing the physico-chemical and mechanical characteristics.

1. Mishra, R. K., Fernández-Carrasco, L., Flatt, R. J. and Heinz, H., A force field for tricalcium aluminate to characterize surface properties, initial hydration, and organically modified interfaces in atomic resolution. *Dalton Trans.*, 2014, **43**, 10602–10616.

2. Brehm, D., Nanoengineered concrete could cut world CO_2. MIT's Department of Civil and Environmental Engineering Brochure, Cambridge, 2007.

3. Allen, A. J., Thomas, J. J. and Jennings, H. M., Composition and density of nanoscale calcium-silicate-hydrate in cement. *Nature Mater.*, 2007, **6**, 311–316.

4. Richardson, I. G., The calcium silicate hydrates. *Cem. Concr. Res.*, 2008, **38**, 137.

5. Dormieux, L. and Ulm, F. J. (eds), *Applied Micromechanics of Porous Materials*, CISM courses and lectures, Springer Wien, New York, 2005.

6. Al-Ostaz, A., Wu, W., Cheng, A. H. D. and Song, C. R., A molecular dynamics and microporomechanics study on the mechanical properties of major constituents of hydrated cement. *Composites: Part B*, 2010, **41**, 543–549.

7. Heinz, H., Lin, T.-J., Mishra, R. K. and Emami, F. S., Thermodynamically consistent force fields for the assembly of inorganic, organic, and biological nanostructures: the INTERFACE force field. *Langmuir*, 2013, **29**, 1754–1765.

8. Dharmawardhana, C. C. and Misra & Wai-Yim Ching, A., Quantum mechanical metric for internal cohesion in cement crystals. *Sci. Rep.*, 2014, **4**, 1–8.

9. Abdolhosseini Qomi, M. J. *et al.*, Combinatorial molecular optimization of cement hydrates. *Nature Commun.*, 2014, **5**, 1–10.

10. Manzano, H., Dolado, J. S. and Ayuela, A., Aluminum incorporation to dreierketten silicate chains. *J. Phys. Chem. B*, 2009, **113**(9), 2832–2839.

11. Pelisser, F., Gleize, P. J. P. and Mikowski, A., Effect of the Ca/Si molar ratio on the micro/nanomechanical properties of synthetic C-S-H measured by nanoindentation. *J. Phys. Chem. C*, 2012, **116**, 17219–17227.

12. Bonaccorsi, E., Merlino, S. and Taylor, H. F. W., The crystal structure of jennite, $Ca_9Si_6O_{18}(OH)_68H_2O$. *Cem. Concr. Res.*, 2004, **34**, 1481–1488.

13. Bonaccorsi, E., Merlino, S. and Kampf, A. R., The crystal structure of tobermorite 14 Å (plombierite), a C-S-H phase. *J. Am. Ceram. Soc.*, 2005, **88**(3), 505–512.

14. Scrivener, K. L. and Kirkpatrick, R. J., Innovation in use and research on cementitious material. *J. Cem. Concr. Res.*, 2008, **38**, 128–136.

15. Scrivener, K. L. and Nonat, A., Hydration of cementitious materials, present and future. *Cem. Concr. Res.*, 2011, **41**, 651–665.

16. Gonzalez-Teresa, R., Dolado, J. S., Ayuela, A. and Gimel, J.-C., Nanoscale texture development of C-S-H gel: a computational model for nucleation and growth. *Appl. Phys. Lett.*, 2013, **103**, 234105.

17. Brooks, C. L., Karplus, M. and Pettit, B. M., *Proteins: A Theoretical Perspective of Dynamics, Structure, and Thermodynamics*, John Wiley, New York, 1988.

18. Frenkel, D. and Smit, B., *Understanding Molecular Simulation: From Algorithms to Applications*, Academic Press Inc, Florida, 1996.

19. Verlet, L., Computer experiments on classical fluids. I. Thermodynamical properties of Lennard-Jones molecules. *Phys. Rev.*, 1967, **159**, 98.

20. Hockney, R. W., The potential calculation and some applications. *Methods Comput. Phys.*, 1970, **9**, 136–211.

21. Al-Ostaz, A., Pal, G., Mantena, P. R. and Cheng, A., Molecular dynamics simulation of SWCNT-polymer nanocomposite and its constituents. *J. Mater. Sci.*, 2008, **43**, 164–173.

22. Shahsavari, R., Buehler, M. J., Pellenq, R. J. M. and Ulm, F. J., First-principles study of elastic constants and interlayer interactions of complex hydrated oxides: case study of tobermorite and jennite. *J. Am. Ceram. Soc.*, 2009, **92**(10), 2323–2330.

23. Jorge Dolado, S. and van Breugel, K., Recent advances in modeling for cementitious materials. *Cem. Concr. Res.*, 2011, **41**, 711–726.